UNIVERSITÄT DUISBURG ESSEN

Offen im Denken

Universität Duisburg-Essen, Institut für Wasserbau und Wasserwirtschaft

H-SAF Associated/Visiting Scientist Activity ref. H-SAF_VSA_13_03

Generic Data Assimilation Test Bed for H-SAF Snow Products and a Conceptual Hydrological Model

Project Report (Draft Final)

Prepared by:

Dirk Schwanenberg (University of Duisburg-Essen, Germany)
Aynur Sensoy (Anadolu University, Eskişehir, Turkey)

Essen, February 2014

Table of Contents

1	**Introduction**	**1**
1.1	Background	1
1.2	Objectives	4
1.3	Tasks and Methods	4
2	**Material and Methods**	**6**
2.1	Overall Framework	6
2.2	Karasu River Basin	6
2.3	RTC-Tools / HBV Implementation	9
2.3.1	Overview	9
2.3.2	Storage Nodes	9
2.3.3	Fluxes	10
2.4	Moving Horizon Estimation (Data Assimilation)	12
2.5	Performance Indicators	13
2.6	Test Bed Integration	13
2.6.1	Overview	13
2.6.2	Data Feeds	14
2.6.3	Data Processing and Analysis	15
2.6.4	Model Workflows	16
2.7	Graphical User Interfaces	17
3	**Experiments and Results**	**18**
3.1	Overview	18
3.2	Model Calibration	18

3.3 Data Assimilation Setup 18

3.4 Data Assimilation Experiments and Results 20

3.4.1 Data Assimilation Inputs / Model Structure 20

3.4.2 Practical benefit of H-SAF products 23

4 Conclusions and Recommendations 25

5 References 26

1 Introduction

1.1 Background

An accurate estimation and monitoring of snow states such as snow coverage and snow water equivalent are important inputs for water resources management. In mountainous regions, data limitations prevent detailed understanding of the variability of snow cover and melt. In situ snowpack measurements are sparsely distributed relative to snowpack heterogeneity leaving much of the hydrologic cycle under-sampled in both time and space (Bales et al. 2006). Moreover, for most mountainous regions, partly due to accessibility constraints, rainfall/snowfall and other meteorological information are often lacking, especially in the highest parts of the catchments. For these reasons, large scale strategies for observing snow properties rely heavily on remote sensing (Schmugge *et al.*, 2002).

Compared to the conventional in situ snow measurements, satellite data are particularly well adapted to the monitoring of snow covered surfaces over continuous space–time scales. A wide range of instruments are available for measuring and observing snow cover; especially, a variety of space borne sensors with various spectral, spatial, and temporal resolutions that purposely meet the needs both required by climatologists and hydrologists.

Snow cover area (SCA) is an important hydrological input for simulating and forecasting the amount of water from snowmelt. The importance of SCA was further accentuated with the studies performed by various researchers to develop and apply runoff models (WMO 1986; WMO 1992). After, regional to global scale satellite-derived estimation of snow cover area became available daily, however, driving models with good SCA estimates remains a challenge in mountainous regions.

Remotely sensed snow covered area information has been used successfully in snowmelt and runoff models (Yang *et al.*, 2003; Tekeli *et al.*, 2005, Clark *et al.*, 2006; Dressler *et al.*, 2006; Kolberg and Gottschalk, 2006; Kolberg *et al.*, 2006; Andreadis and Lettenmaier, 2006; Udnaes *et al.*, 2007; Parajka and Blöschl, 2008). Remotely sensed snow water equivalent has also been used in the models (Derksen *et al.*, 2003; Andreadis and Lettenmaier, 2006; Pulliainen, 2006, Hall and Riggs, 2007; Dong *et al.*, 2007).

The runoff prediction studies incorporate SCA as a major and sensitive input into operational models that relate snow distributions to snowmelt runoff generation or as a means of updating hydrologic model snowpack simulations and checking the internal validity of snowmelt runoff model (Andreadis and Lettenmaier 2006; Clark et al. 2006; Dressler et al. 2006; McGuire et al. 2006; Şorman et al. 2009). The only widely applied model optimized for direct input of remotely sensed SCA data is the Snowmelt Runoff Model, SRM, in which snowmelt is calculated from SCA derived by means of remote sensing. With the widespread application of satellite data for monitoring snow accumulations, the model has been refined over a period of time (Martinec 1975; Martinec *et al.*, 1983; Rango and Vankatwijk, 1990;

Rango and Martinec 1995; Mitchell and DeWalle, 1998; Richard and Gratton, 2001; Gomez and Rango, 2002, Lee *et al.*, 2005; Tekeli et al. 2005a; Nagler *et al.*, 2008; Li *and Williams*, 2008; Martinec *et al*. 2008; Xingong and Williams, 2008; Immerzeal et al., 2009; Boudhar *et al.*, 2009; Jain et al. 2010; Butt and Bilal, 2011; Tahir et al, 2011).

Ideally, a system that optimally combines snow information from both remote sensing and modelling predictions and at the same time accounts for the limitations of each should provide estimates that are superior to those derived from either models or remote sensing alone. This method is commonly known as data assimilation (McLaughlin, 1995).

Data assimilation in hydrological models is a relatively recent advance, but one which has been enthusiastically taken up, with various approaches being used: refer to recent reviews by Reichle (2008) and Liu et al. (2012), and references therein. The feasibility of undertaking spatially distributed data assimilation in hydrological models has been demonstrated by a number of recent studies. (McMillan et al. (2013). The observations used to update model states can include river flows (Seo et al., 2003), soil moisture (Parajka et al., 2006; Brocca et al., 2010; Flores et al., 2012), snow-covered area and snow water equivalent (Clark et al., 2006; Zaitchik and Rodell, 2009; Andreadis and Lettenmaier, 2006), and satellite observations of discharge (Neal et al., 2009; Andreadis et al., 2007). Joint use of different observation types is also possible. For example, Aubert et al. (2003) assimilated streamflow and soil moisture observations. The model states that are updated include in-channel water volume (Ricci et al., 2011), soil water (Lee et al., 2011), groundwater (Zhou et al., 2011; Clark et al., 2008) and snow water equivalent (De Lannoy et al., 2012; Slater and Clark, 2006).

Data assimilation methods have been applied in hydrology with increasing frequency in recent years. There are several different data assimilation techniques, but the most commonly used are the variational assimilation and variants of the Kalman filter (KF). The former is essentially an optimization procedure that adjusts uncertain variables and/or parameters to obtain the best fit to observations.

Snow cover observations have been used through various assimilation methods, including rule based updating (Rodell and Houser, 2004; Hall *et al.*, 2010), Bayesian filtering (e.g., Kolberg and Gottschalk, 2006; Kolberg *et al.*, 2006) nudging forcing fields toward likely precursors of the observed snow cover area (Zaitchik and Rodell, 2009) and Kalman and ensemble Kalman filter (EnKF) methods (Andreadis and Lettenmaier, 2006; Clark *et al.*, 2006; Su *et al.*, 2008; Kumar *et al.*, 2008).

Data assimilation is a key element of real-time flood forecasting (Madsen et al., 2000), and most forecasting systems apply some form of data assimilation. The primary goal of data assimilation is to guarantee an up-to-date representation of the state variables in model terms, making use of most recent available measurements. The new state is then used as an initial state for subsequent forecasts. Most implementations of these sequential data assimilation

methods however are custom implementations specially designed for, and integrated with the code of a particular model. This is probably a consequence of the lack of generic data assimilation software packages and tools. The use of such custom implementations has a number of disadvantages, first both the development and the implementation of these methods is time consuming and expensive and it is hard to reuse these data assimilation methods and tools for other models than for which they have originally been developed for.

Operational forecasting of river flow is becoming overly important and prevalent to get an answer for several subjects, for instance developing early warning of floods, prediction of low flow for navigation or water resources prediction for operating reservoirs. Besides, the H-SAF vision for CDOP-2 relies on the assumption that H-SAF supports providing products and services in support of Operational Hydrology. This approach aims to accomplish the added value of satellite derived products in operational streamflow forecasting through hydrological models. In CDOP-2 Phase, it is intended to develop or complement interface products for assimilating existing hydrological models, developing tools which will allow models to accept soil moisture and/or snow cover products. Another purpose is to provide an efficient user support and training, as well as a viable communication with user communities. Therefore, a generic software package for data assimilation would be helpful for the H-SAF hydrology community, so that it is possible to apply data assimilation methods for existing and new models prefered by hydrology teams.

Therefore, one of the objectives of this study is the implementation of a generic data assimilation test bed, which enables a modular integration of modelling components into data assimilation procedures and data model integration platforms. Therefore, the modelling layer will depend on open source model libraries such as developed in Schwanenberg, 2012. The data assimilation component will alternatively link to platform such as Matlab for prototyping new assimilation algorithms or dedicated existing open platforms for data assimilation such as OpenDA (http://www.openda.org). Pre- and post-processing of remote sensing data may rely on open platforms such as Delft-FEWS (oss.deltares.nl/web/delft-fews) (Werner et al., 2013) or others. The main objective of this activity is the technical integration and exemplary application of the modular framework.

Several snow modeling and monitoring studies have been carried out in the Upper Euphrates Basin which is the main mountainous test site for Turkey. Several studies were performed to validate snow products such as SCA or SWE of different satellites (e.g. MODIS, NOAA-AVHRR, SEVIRI, etc) (Şorman and Beşer, 2011; Şorman et al., 2007; Tekeli et al., 2006) and moreover several hydrological model application studies were carried out using these products (Şensoy et al. 2012, Şensoy and Uysal, 2012; Şorman et al., 2009; Sensoy et al., 2006, Tekeli et al., 2005). Therefore, using the experiences on monitoring and hydrological modelling in this test site would be applicable for operational runoff forecasting

with NWP data, the results can be compared with and without data assimilation either for different snow products of HSAF or different satellite products.

1.2 Objectives

The main objectives of this VS activity are:

- Implement a modular test bed with generic software for data assimilation of HSAF snow products (H10 and H13) in application to conceptual hydrological models
- Enable the performance testing of H-SAF snow products (H10 and H13) and data assimilation for improving the lead time accuracy of operational forecasts together with Numerical Weather Prediction Data (NWP)
- Enable the performance comparison of H-SAF snow products (H10 and H13) to other satellite data (MODIS)
- Test and deploy a data-model integration platform that can be adaptable for different data inputs including satellite products and various hydrological models for making H-SAF products easier available to a large user community

1.3 Tasks and Methods

The visiting scientist activity consists of the following tasks:

- Draft the conceptual and technical specification of the modular data assimilation test bed in terms of the model, DA and data model integration components as well as related interfaces
- Integrate a prototype of the data assimilation test bed with selected available components according to the specifications above
- Apply the test bed for implementing a snow assimilation procedure based on the snow products H10 and H13 for the test basin (Upper Euphrates Basin) in Turkey
- Setup a procedure for the lead-time performance assessment of the assimilated model in combination with NWP and compare results against other H-SAF test site, probably the Upper Main sub-basin in Germany provided by Bundesanstalt für Gewässerkunde (BfG), Koblenz, Germany
- Document results and give guidelines for extending the test bed to larger basins, make use of the interfaces

The host integrated additional satellite-based snow cover data into the modeling frame to compare results with and without assimilation procedure.

The visiting scientist activity was implemented by two trip of Dr. Dirk Schwanenberg (University of Duisburg-Essen) to Anadolu University in Turkey (Aynur Sensoy & co-workers):

- Trip 1: November 27-29, 2013,
- Trip 2: January 20-22, 2014

and additional back-office support.

2 Material and Methods

2.1 Overall Framework

The implementation of the data assimilation framework consists of three exchangeable layers:

- Delft-FEWS (Werner et al., 2013, http://oss.deltares.nl/web/delft-fews) is used for the implementation of the **Data-Model Integration** layer. The task of this component is to import data from different sources into a homogeneous database, validate and pre-process the data for the models, run the models and implement various hindcasting experiments, visualize data and model results and assess the model and forecast performance. The software is freely available on: oss.deltares.nl/web/delft-fews
- The **Data Assimilation** layer is implemented in RTC-Tools (http://oss.deltares.nl/web/rtc-tools), an open source package originally developed for real-time control applications. The specific DA technique we use is Moving Horizon Estimation (MHE). This specific technique requires an implementation of the hydrological model in the RTC-Tools model library. An alternative for arbitrary model is the OpenDA (http://www.openda.org/joomla/index.php) package including a variety of Kalman Filters.
- The **Model Library** layer is based on the model library of RTC-Tools. Besides the reimplementation of the HBV model, it includes several other hydrological models and a more generic framework for arbitrary conceptual hydrological model in development at Deltares.

The Delft-FEWS Published Interface format (PI-XML) enables the communication between the different layers and enables the exchange of a specific component against another one, see check the following website for a description of the interface:

http://publicwiki.deltares.nl/display/FEWSDOC/The+Delft-Fews+Published+Interface

The compliance of a model with the PI interface requires a so-called Model Adapter which is available for many commonly used hydrological models, check

https://publicwiki.deltares.nl/display/FEWSDOC/Models+linked+to+Delft-Fews

NB:

We give preference to the joint implementation of Data Assimilation and Model Library in the RTC-Tools package mainly because of performance reasons and the more suitable MHE technique. The drawback of this concept is the need for a reimplementation of the modeling component in the RTC-Tools model library compared to the combination of OpenDA and arbitrary hydrological models connected with the PI-XML interface.

2.2 Karasu River Basin

Snow plays a crucial role in the headwaters of Euphrates River Basin as in many other mountainous regions. Snowmelt contributes up to 60-70% of the annual volume of runoff in

the Upper Euphrates River Basin (Karasu Basin), during spring and early summer months. The prediction of snowmelt-induced runoff at the outlet of Karasu Basin has a great potential especially for application in flood forecasting, reservoir management, irrigation, hydropower generation, water supply, since five large dam reservoirs exist at the downstream of the basin. Karasu Basin, as one of the major upstream tributaries of Euphrates River, is located at the eastern part of Turkey. Fig. 1 shows the location of the basin with its river network. Karasu Basin boundaries are within the longitudes 38° 58' E to 41° 39' E and latitudes 39° 23' N to 40° 25' N (Fig. 1). The basin has a drainage area of 10 275 km^2 and ranges in altitude from 1125 to 3487 m above sea level. The basin with an elevation map is provided in Figure 2. The main land cover types are pasture, shrub, grass and wasteland.

In the present study, the basin is divided into ten elevation zones with equal areas of 10% (Table 1) to carry out snowmelt runoff studies. Hypsometric mean elevations of the zones are provided in Table 2.

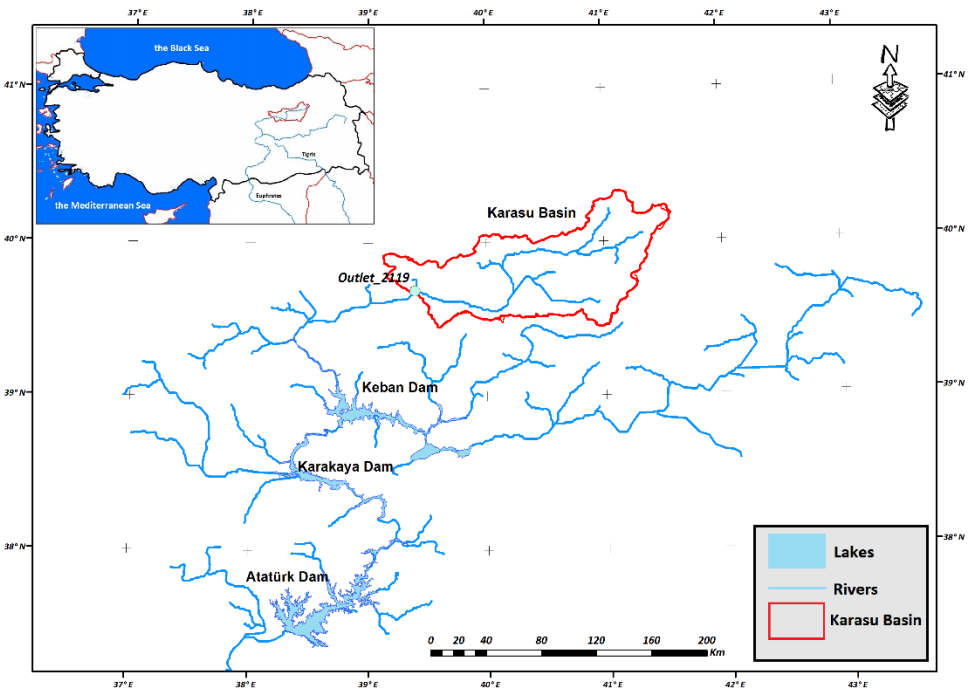

Figure 1 Location of the Upper Euphrates Basin in Turkey

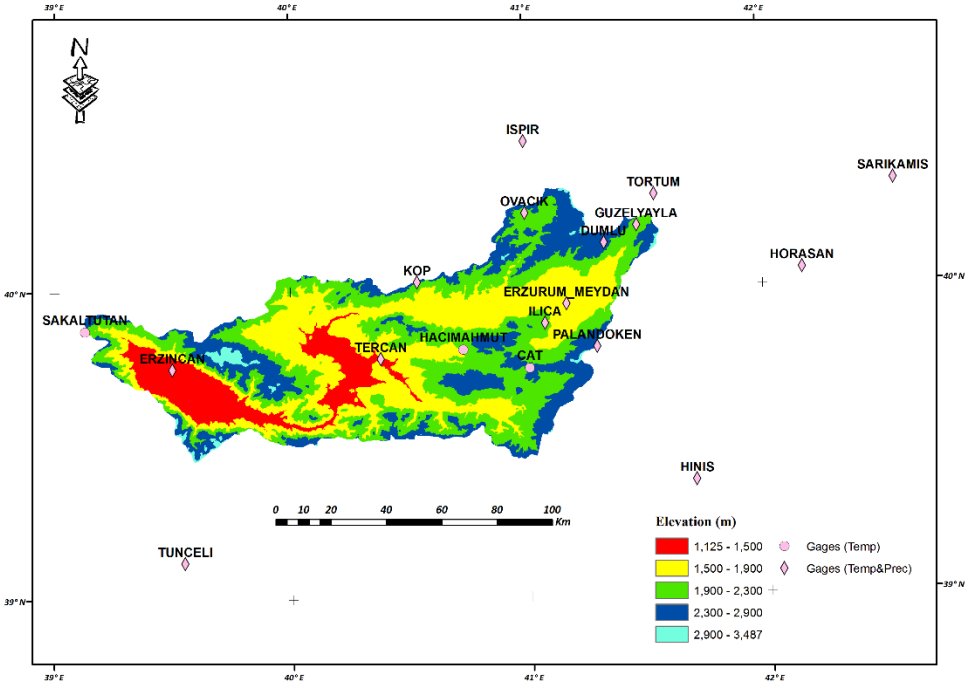

Figure 2 Elevational zones and meteorological gaging network of the Upper Euphrates Basin (Karasu Basin)

Table 1 Hypsometric mean elevation of the basin and elevation zones for the Upper Euphrates Basin

Zone	Area [km^2]	Area [%]	Mean Elevation [m]
1	1027.5	10	1314
2	1027.5	10	1584
3	1027.5	10	1732
4	1027.5	10	1829
5	1027.5	10	1930
6	1027.5	10	2045
7	1027.5	10	2163
8	1027.5	10	2286
9	1027.5	10	2446
10	1027.5	10	2993
Total	**10275.0**	**100**	**1983**

2.3 RTC-Tools / HBV Implementation

2.3.1 Overview

Conceptual hydrological models such as HBV-96 (Lindstrom, 1997) have been the workhorse of operational forecasting systems for decades. Deltares (The Netherlands), the Federal Institute of Hydrology (BfG, Germany) as well as the Federal Office for the Environment (FOEN, Switzerland) apply the model for many years within the operational forecasting system of River Rhine. Recent research (Weerts et al., 2010) aims at improving the model's lead time accuracy by data assimilation procedures based on several version of the Kalman Filter.

This work relies on a reimplementation of the original HBV model in the open source software package RTC-Tools (oss.deltares.nl/web/rtc-tools). Therein, the standard simulation mode has been extended by a so-called adjoint mode based on reverse algorithmic differentiation for computing first-order model sensitivities. This enables the application of variational data assimilation approaches such as the Moving Horizon Estimation (Schwanenberg et al., 2012) we also use in this research.

2.3.2 Storage Nodes

Storage nodes are represented by a mass balance according to

$$s^k = s^{k-1} + \Delta t \sum_i Q_i^k (s^k, s_i^k) \tag{1}$$

where s is the storage, Q the discharge of links between storage nodes, the index i denotes the link to a neighboring storage node. Table 2 gives a summary of storage nodes in the HBV model.

Table 2 Overview of HBV Storage Nodes

ID	Name	Description
SP	Snow Pack	Snow Water Equivalent [mm] of the snow pack of the snow component
WC	Water Content in Snow	Water Content [mm] in snow pack of the snow component
IC	Interception	Interception Storage [mm] of vegetation of the interception component
SM	Soil Moisture	Soil Moisture [mm] of the soil component
UZ	Upper Zone Storage	Upper Zone Storage [mm] of the response component
LZ	Lower Zone Storage	Lower Zone Storage [mm] of the response component

2.3.3 Fluxes

Fluxes represent the flow Q from node 1 to another node 2 according to

$$Q^k(s_1^k, s_2^k, p, d^k) \tag{2}$$

where s_1 and s_2 are the storage volumes of the two nodes. The flux calculation may depend on additional parameters p and external time series d. Depending on the characteristics of the link, the nodes are optional if water enters or leaves the model, for example in case of the actual evaporation which is extracted from the soil moisture storage. Fluxes without both upstream and downstream nodes are intended for pre- and post processing independent of the storage nodes.

The output of a flux component is either the unit volume q [mm/time step] or the discharge Q [m^3/s]. Table 3 gives a summary about the HBV fluxes

Table 3 Overview of HBV Fluxes

ID	Description	RTC-Tools / HBV-96 flux implementation
RF	Rainfall from precipitation for pre-processing	$q = \begin{cases} 0 & \text{if } T \le TT - \frac{TTI}{2} \\ RFCF \frac{T - TT - \frac{TTI}{2}}{TTI} P & \text{if } TT - \frac{TTI}{2} < T < TT + \frac{TTI}{2} \\ RFCF\, P & \text{if } T \ge TT + \frac{TTI}{2} \end{cases}$
SF	Snowfall from precipitation for pre-processing	$q = \begin{cases} SFCF\, P & \text{if } T \le TT - \frac{TTI}{2} \\ SFCF \left(1 - \frac{T - TT - \frac{TTI}{2}}{TTI} \right) P & \text{if } TT - \frac{TTI}{2} < T < TT + \frac{TTI}{2} \\ 0 & \text{if } T \ge TT + \frac{TTI}{2} \end{cases}$
EP	Correction of potential evaporation	$q = ECORR\ EPM \left(1 + ETF \frac{T - TM}{TM} \right)$
MELT	Snow melt from snow pack into water content SP -> WC	$q = \begin{cases} 0 & \text{if } T \le TTM \\ \min(CFMAX\ TFAC\ (T - TTM), SP + SF) & \text{if } T \ge TTM \end{cases}$
REFR	Refreezing from water content into snow melt	$q = \begin{cases} \min(-CFR\ CFMAX\ TFAC\,(T - TTM), WC + RF) & \text{if } T \le TTM \\ 0 & \text{if } T \ge TTM \end{cases}$

ID	Description	RTC-Tools / HBV-96 flux implementation
	WC -> SP	
IN	Release from water content storage WC ->	$q = \begin{cases} WC - CHW\ SP & \text{if } WC > CHW\ SP \\ 0 & \text{if } WC \le CHW\ SP \end{cases}$
EI	Evaporation from interception storage IC ->	$q = \begin{cases} EP & \text{if } IC > EP \\ IC & \text{if } IC \le EP \end{cases}$
INI	Release from interception storage IC ->	$q = \begin{cases} IC - LIC & \text{if } IC > LIC \\ 0 & \text{if } IC \le LIC \end{cases}$
EA	Actual evaporation from soil moisture storage SM ->	$q = \begin{cases} \frac{SM}{LP\,FC} EP* & \text{if } SM < LP\,FC \\ EP* & \text{if } SM \ge LP\,FC \end{cases}$ * if interception is used, EP needs to get reduced by EI
R	Soil runoff from soil moisture to upper zone storage SM -> UZ	$q = \left(\frac{SM}{FC}\right)^{BETA} IN$
CF	Capillary Flow from upper flow to soil moisture storage UZ -> SM	$q = TFAC\ CFLUX \left(1 - \frac{SM}{FC}\right)$
PERC	Percolation from upper to lower zone storage UZ -> LZ	$q = \begin{cases} UZ & \text{if } UZ < TFAC\ PERC \\ TFAC\ PERC & \text{if } UZ \ge TFAC\ PERC \end{cases}$ Upper storage is checked for the availability of sufficient water
Q0	Upper zone release UZ ->	$q = TFAC\ K\ UZ^{1+ALPHA}$
Q1	Lower Zone release	$q = TFAC\ K1\ LZ$

ID	Description	RTC-Tools / HBV-96 flux implementation
	LZ ->	
Q	Post processing for adding individual releases	$Q = \frac{AREA}{\Delta t} \sum_i q_i$

2.4 Moving Horizon Estimation (Data Assimilation)

Our dedicated implementation of the HBV model follows an implementation according to

$$x^k = f(x^{k-1}, d^k, u^k) \tag{3}$$

$$y^k = g(x^k, d^k, v^k) \tag{4}$$

where x, y, d are the state, output and external forcing vectors, respectively, u, v are noise terms, $f(), g()$ are functions representing arbitrary linear or nonlinear components of the HBV model and k is the time step index.

Based on Eq. (3)-(4) above, we formulate the Moving Horizon Estimation (MHE) for a forecast time $k = 0$ over an assimilation period $k = [-N+1, 0]$ of $N \geq 1$ time steps by an optimization problem according to

$$\min_{u,v} \sum_{k=-N+1}^{0} w_x \left\| \hat{x}^k - x^k(u) \right\| + w_y \left\| \hat{y}^k - y^k(u,v) \right\| + w_u \left\| u^k \right\| + w_v \left\| v^k \right\| \tag{5}$$

$$\text{subject to} \quad u_L \leq u^k \leq u_U \qquad v_L \leq v^k \leq v_U \tag{6}$$

where $\hat{x}^k, \hat{y}^k$ are observations of the state and the dependent variable vectors, $\| \ \|$ is a suitable norm penalizing the deviation between observed and simulated quantities and the introduction of noise by the data assimilation procedure, $w_{u,v,x,y}$ are weighting coefficients for defining the trade-off between different penalties. Furthermore, the noise terms get bounded by inequality constraints. For the sake of simplicity, our formulation considers constant bounds only.

The key to the efficient solution of the optimization problems above, in particular in operational applications with runtime restrictions, is the computation of the derivatives of the objective function we refer to as $J(u,v)$ for applying gradient-based optimizers such as IPOPT (Wächter & Biegler, 2006). Since numerical differentiation is a computational burden for larger optimization problems and introduces truncation errors, we rely on adjoint modelling based on algorithmic differentiation in reverse mode (Griewank & Walther, 2008) for tracing back first-order derivatives backwards in time through the model.

2.5 Performance Indicators

Performance indicators play an essential role in the evaluation of the assimilation procedure. We distinguish the assessment of model performance and forecast lead time performance. The first one is used for model calibration and validation, but also indicates how much the assimilation procedure is pushing the model towards the observation. We use

$$BIAS = \frac{1}{N}\sum_{k=1}^{N}(x^k - y^k) \tag{7}$$

$$RMSE = \sqrt{\frac{1}{N}\sum_{k=1}^{N}\left(x^k - y^k\right)^2} \tag{8}$$

$$R2 = \frac{\sum_{k=1}^{N}(x^k - \overline{x})(y^k - \overline{y})}{\sqrt{\sum_{k=1}^{N}(x^k - \overline{x})^2}\sqrt{\sum_{k=1}^{N}(y^k - \overline{y})^2}} \tag{9}$$

$$NSE = 1 - \frac{\sum_{k=1}^{N}(y^k - x^k)^2}{\sum_{k=1}^{N}(y^k - \overline{y})^2} \tag{10}$$

where *BIAS* is the bias between simulation x^k and observation y^k, *RMSE* is the Root Mean Square Error, *R2* is the correlation coefficient and *NSE* is the Nash-Sutcliffe model efficiency.

For assessing the forecast lead time accuracy, we reformulate the *BIAS*, *RMSE* and *R2* indicators in Eq. (7)-(9) to

$$BIAS^L = \frac{1}{N}\sum_{k=1}^{N}(x^{k,L} - y^k) \tag{11}$$

where L is the forecast lead time we want to assess and the value $x^{k,L}$ indicates the value of a forecast with a forecast time of $k - L$.

2.6 Test Bed Integration

2.6.1 Overview

The test bed integration relies on the software tools Delft-FEWS (oss.deltares.nl/web/delft-fews). The software was originally developed by Deltares for integrating flood forecasting and flood early warning, providing a sophisticated collection of generic modules designed for building a system customized to the specific requirements of an individual agency. During over 10 years of development, the flexible nature of the system has led to include applications for water resources, drought forecasting, water quality forecasting and real time control. The

philosophy of Delft-FEWS is to provide an open shell system for managing the forecasting process. Delft-FEWS incorporates a wide range of general data handling utilities, while providing an open interface to any external calculation model. The modular and highly configurable nature of Delft-FEWS allows it to be used effectively both in simple systems and in highly complex systems utilizing the full range of hydrological and hydraulic modeling. Delft-FEWS can either be deployed in a stand-alone, manually driven environment, or in a fully automated distributed client-server environment. In the context of this research, we use the software for integrating the test bed with data feeds for observed data from meteorological and streamflow gauges, H-SAF and alternative remote sensing products and Numerical Weather Predictions (NWP) in combination with internal data validation / processing tools and the external RTC-Tools / HBV model with the data assimilation procedure.

2.6.2 Data Feeds

Table 4 provides a summary of the configured data feeds in the test bed. Within these data feeds, the data is imported, placed at a consistent spatial reference and validated for missing data and outliers.

Table 4 Data Feeds

Data Feed	Format	Description
ImportExcelCSV	csv	meteorological and streamflow gauges, (sub-)catchment averages forcing (precipitation & temperature) for the model, observed discharge data
ImportHSAF	ESRI ASCII, GRIB, GRIB2	H-SAF products H10 (snow covered area, clipped and converted from buffer to ESRI ascii format), H12 (fractional snow coverage), H13 (snow water equivalent) and H14 (soil moisture)
ImportMODIS	csv	Pre-processed MODIS data: basin-averaged fractional snow coverage

Screenshots of the spatial H-SAF data is presented in Figure 3.

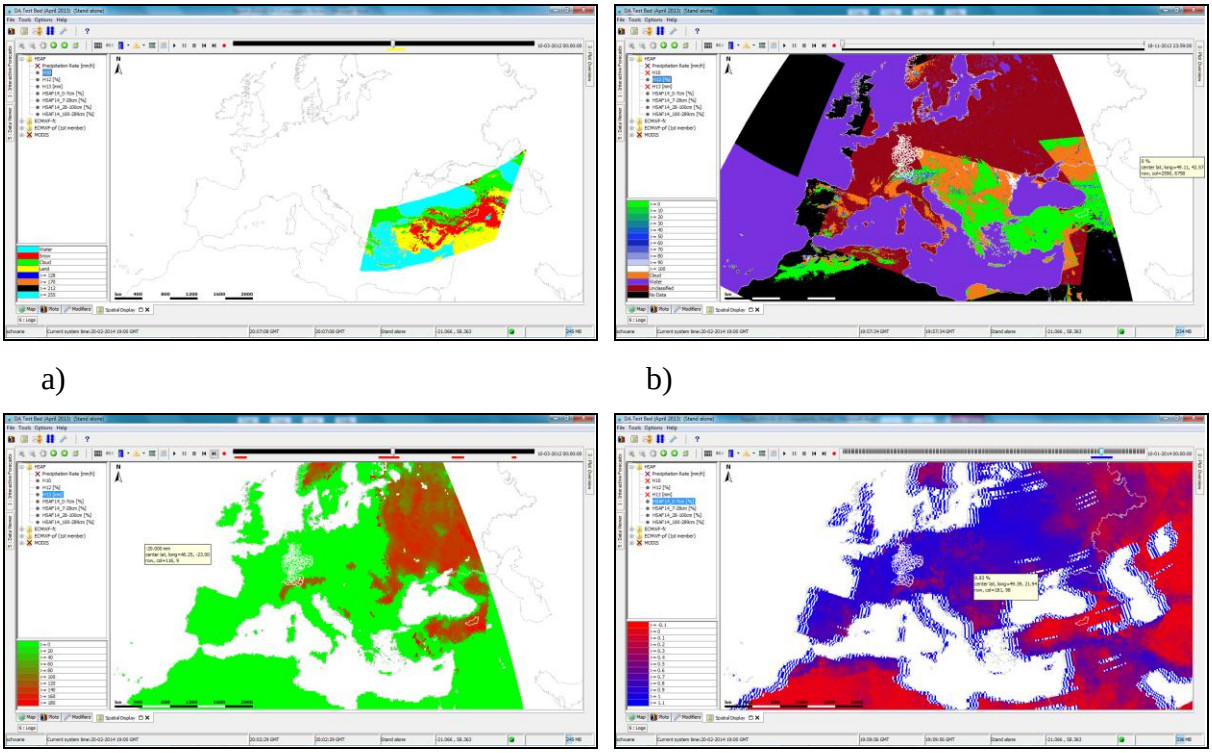

a) b)

c) d)

Figure 3 Screenshots of H-SAF products a) H10, b) H12, c) H13, d) H14

A remaining issue of the data feeds is the import of H-SAF/H14. Figure 3 shows obvious data errors at the coastal regions. The identification and solution of this problem is pending.

2.6.3 Data Processing and Analysis

Data processing has been primarily implemented for H-SAF products:

- The **H10** snow mask (snow / no-snow / cloud) is converted to a fractional snow coverage on the spatial extent of the river basins (alternatively on the level of sub-basins). It is computed as the ratio between snow covered pixels and the total number of pixels with snow and no-snow information. The ratio is only accepted, if the number of visible pixels is up-crossing a pre-defined threshold (see Figure 4). A preprocess is carried out to eliminate the data with cloud coverage higher than 25 % of all area.
- The **H13** snow water equivalent is spatially aggregated to the basin.

Figure 4 Fractional Snow Coverage of Karasu basin from Modis and the processed H-SAF / H10

2.6.4 Model Workflows

The RTC-Tools / HBV model is implemented in the test bed by using the Delft-FEWS General Model Adapter and the PI-XML format definition, see

https://publicwiki.deltares.nl/display/FEWSDOC/The+Delft-Fews+Published+interface+(PI)

We distinguish different model applications for which we configure separate model workflows in the test bed:

1) Update

   The "Update" workflow runs a model simulation with observed forcing (precipitation and temperature). It is the baseline for the assessment of the model performance and the model calibration and validation.

2) Update DA

   The "Update DA" workflow runs a model simulation with observed forcing and additional data for the data assimilation (observed discharge, remote sensing data etc.). The purpose of the DA workflow is the preparation of system state for the forecast workflow.

3) Forecast

   The forecast workflow picks up the system state from the Update workflow with and

without DA and computes a streamflow forecast. We distinguish between forecasts with perfect forcing based on observed data (for neglecting the meteorological uncertainty) and forecasts with NWP.

4) Performance Runs

The performance runs assess the model performance (Bias, RMSE, R2, NSE) of the Update run and the lead time performance (Bias, RMSE, R2 for different lead times) of the Forecast runs.

2.7 Graphical User Interfaces

This Section presents the most important Graphical User Interfaces of the test bed:

- The Modifier Display (Figure 5) of the Interactive Forecasting Displays enables the definition of variables bounds and weighting factors of the MHE.

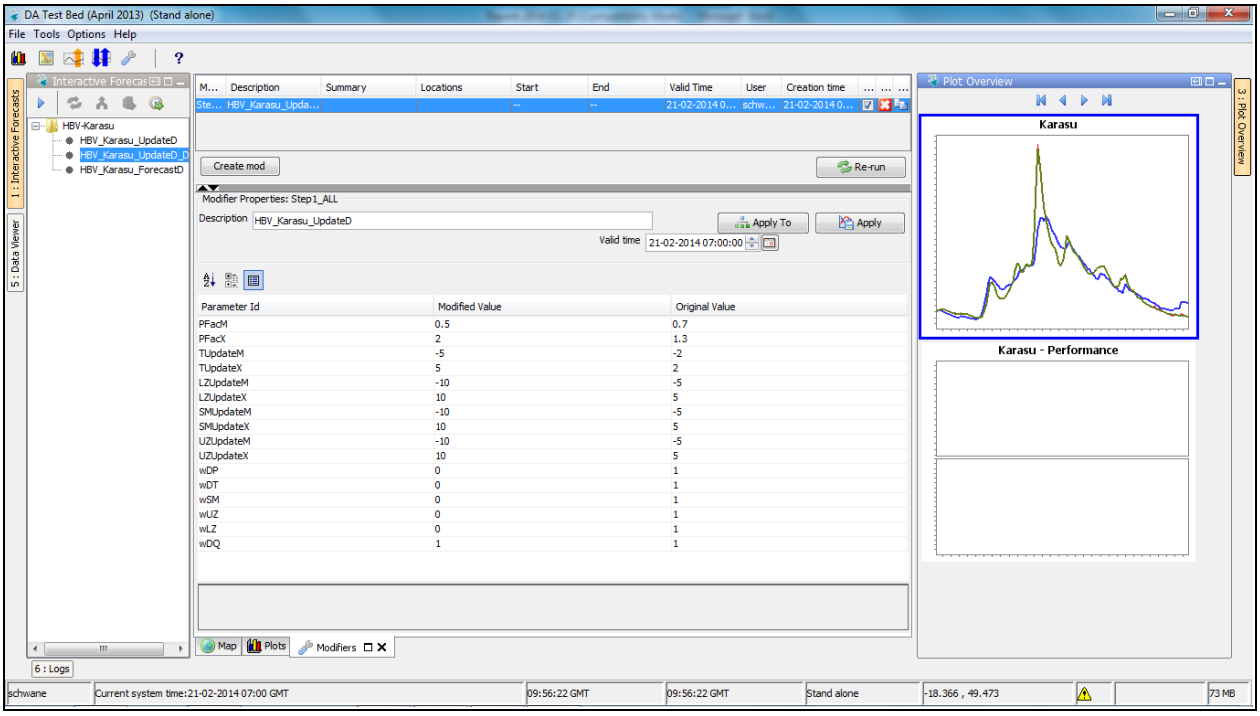

Figure 5 Interactive Updating and Forecasting: Modifier Display for the definition of variables bounds and weighting factors of the MHE

3 Experiments and Results

3.1 Overview

This Chapter describes the model calibration, the setup of the data assimilation procedure and the configured data assimilation experiments with preliminary results. The latter verify the implementation of the data assimilation by

- assessing the impact of the choice of the DA inputs (precipitation, temperature) and states (soil moisture, upper and lower zone storage terms) as well as the model structure on the potential assimilation of the simulated runoff,
- evaluating the practical benefit of the H-SAF data products for improving the forecast accuracy of streamflow forecasts.

3.2 Model Calibration

For the model calibration, we use the RTC-Tools / Matlab interface to externalize the model parameters and to conduct an automatic model calibration by optimization. In Table 5, we present the achieved model performance of the Karasu model in comparison to the performance of the model of the upper Main catchment in Germany.

Table 5 Model calibration performance

Basin	Mean Flow	Calibration (Karasu: Oct 2000 – Sep 2008) (Main 1961 – 2006)				Validation (Karasu: Oct 2008 – Sep 2012)			
	Q [m^3/s]	BIAS [m^3/s]	RMSE [m^3/s]	R2 [-]	NSE [-]	BIAS [m^3/s]	RMSE [m^3/s]	R2 [-]	NSE [-]
Karasu	85.14	-1.49	33.22	0.843	0.839	-6.69	34.07	0.746	0.736
Main1	31.05	-0.07	11.12	0.912	0.912	-	-	-	-

The R2 and NSE performance indicators of the Karasu model are about 0.1 lower than the ones of the Main model. We suspect the reason for this in the sparse data availability in the Karasu basin and the dominant snow accumulation and melting processes. Therefore, this basin should have some potential for improvement in combination with the data ssimilation procedure.

3.3 Data Assimilation Setup

The MHE data assimilation procedure can modify both model inputs and states (Table 6) of the HBV model. In this research, we apply it to the model inputs precipitation (P) and

temperature (*T*) as well as the model states soil moisture (*SM*), upper zone storage (*UZ*) and lower zone storage (*LZ*). The precipitation is modified by a factor in the bounds 0.7 – 1.3. All other variables are implemented as increments of the current value. The increments are bounded in the range of +/- 1 K for the temperature and +/- 1 mm for *SM*, *UZ* and *LZ*.

Table 6 Optimization variables and bound constraints

Optimization Variable	**Bound Constraints**
Precipitation Factor (P_f)	$0.7 \le P_f^k \le 1.3$
Temperature (ΔT^k)	$-1K \le \Delta T^k \le 1K$
Soil Moisture Update (Δs_{SM}^k)	$-1\text{mm} \le \Delta s_{SM}^k \le 1\text{mm}$
Upper Zone Update (Δs_{UZ}^k)	$-1\text{mm} \le \Delta s_{UZ}^k \le 1\text{mm}$
Lower Zone Update (Δs_{LZ}^k)	$-1\text{mm} \le \Delta s_{LZ}^k \le 1\text{mm}$

The data assimilation by Moving Horizon Estimation (MHE) allows a flexible definition of metrics for penalizing the introduction of noise to the model, i.e. the change of model inputs and states, and the disagreement of observed and simulated quantities. For simplicity, we start with penalizing both noise and disagreement by quadratic norms. This means that the deviation is penalized in a least-square sense. The weighting coefficients define the trade-off between the introduction of noise and the disagreement of the observed and simulated data (Table 7). They can be used to fine-tune the MHE: If we know that the temperature includes only a small amount of uncertainty, we apply a larger weighting factor to the temperature change to enforce a close agreement of observed and assimilated temperature.

Table 7 Objective function terms by variable

Variable		Objective Function Term
Model Inputs	Precipitation (*P*)	$w_P(\Delta P^k)^2$
	Temperature (*T*)	$w_T(\Delta T^k)^2$
Model States	Snow Water Equivalent (*SWE* = *SP* + *WC*)	$w_{SWE}(\hat{s}^k_{SWE} - s^k_{SWE})^2$
	Soil Moisture (*SM*)	$w_{SM}(\hat{s}^k_{SM} - s^k_{SM})^2 + w_{\Delta SM}(\Delta s^k_{SM})^2$
	Upper Zone Storage (*UZ*)	$w_{\Delta UZ}(\Delta s^k_{UZ})^2$
	Lower Zone Storage (*LZ*)	$w_{\Delta LZ}(\Delta s^k_{LZ})^2$
Model Outputs	Snow Covered Area (*SCA*)	$w_Q(\mathrm{A}^k_{SCA} - A^k_{SCA})^2$
	Discharge (*Q*)	$w_Q(\hat{Q}^k - Q^k)^2$

3.4 Data Assimilation Experiments and Results

3.4.1 Data Assimilation Inputs / Model Structure

This experiment is intended to assess the impact of the choice of the DA inputs (*P*, *T*) and states (*SM*, *UZ*, *LZ*) as well as the model structure on the potential assimilation of the simulated runoff. In a first step, we apply the data assimilation to the simulation period of the model calibration and validation. The assimilation runs are setup such that precipitation, temperature etc. are used separately in individual runs and together in a joint run. We put a high weighting on the agreement of observed and simulated discharges and a low one on the introduced noise to assess the maximum discharge agreement for each run. Table 11 and Table 10 summarize the results for the calibration periods of the Karasu and Main1 models. Table 10 presents the results for the validation period of Karasu model.

Table 8 **Karasu:** Model performance of simulation run without data assimilation in comparison to run with different data assimilation setups (calibration period)

Run	Mean Flow	Model Performance (Oct 2000 – Sep 2008)			
	Q [m^3/s]	BIAS [m^3/s]	RMSE [m^3/s]	R2 [-]	NSE [-]
without DA	84.99	-1.49	33.22	0.843	0.839
DA (ΔP)	84.99	-1.51	19.05	0.948	0.947
DA (ΔT)	84.99	-2.82	15.61	0.966	0.965
DA (Δs_{SM})	84.99	-0.10	16.33	0.961	0.961
DA (Δs_{UZ})	84.99	0.77	9.38	0.987	0.987
DA (Δs_{LZ})	84.99	1.34	21.32	0.934	0.934
DA (ALL)	84.99	-0.06	3.58	0.998	0.998

Table 9 **Main1:** Model performance of simulation run without data assimilation in comparison to run with different data assimilation setups (calibration period)

Run	Mean Flow	Model Performance (Jan 1962 – Dec 2006)			
	Q [m^3/s]	BIAS [m^3/s]	RMSE [m^3/s]	R2 [-]	NSE [-]
without DA	31.05	-0.07	11.12	0.912	0.912
DA (ΔP)	31.05	-0.013	5.99	0.974	0.974
DA (ΔT)	31.05	-0.123	6.879	0.966	0.966
DA (Δs_{SM})	31.05	0.005	6.544	0.969	0.969
DA (Δs_{UZ})	31.05	0.323	4.283	0.987	0.987
DA (Δs_{LZ})	31.05	0.164	5.749	0.976	0.976
DA (ALL)	31.05	0.023	1.509	0.998	0.998

Table 10 Model performance of simulation run without data assimilation in comparison to run with different data assimilation setups (validation period)

Run	Mean Flow	Model Performance (Oct 2008 – Sep 2012)			
	Q [m^3/s]	BIAS [m^3/s]	RMSE [m^3/s]	R2 [-]	NSE [-]
without DA	81.84	-6.69	34.07	0.746	0.736
DA (ΔP)	81.84	-2.69	15.22	0.950	0.947
DA (ΔT)	81.84	-22.16	31.77	0.885	0.769
DA (Δs_{SM})	81.84	-0.70	12.76	0.963	0.963
DA (Δs_{UZ})	81.84	1.50	7.14	0.989	0.988
DA (Δs_{LZ})	81.84	-0.23	16.88	0.935	0.935
DA (ALL)	81.84	-0.04	2.35	0.999	0.999

One conclusion from Table 8 - Table 10 is the proper technical functioning of all individual assimilation runs. The R2 and NSE performances for the Karasu model are improved from 0.843/0.839 to a minimum value of 0.934 in the calibration period. The R2 and NSE performances are improved from 0.746/0.736 to a minimum value of 0.935 in the validation period except for the run with the modification of the temperature input, the mass balance of all other runs is improved significantly. This is not a surprise, since all of these runs, except for the one with temperature input, directly modify the mass balance of the model. The performance in the Main1 basin is very similar.

Another important conclusion is that the assimilation gets the simulated discharge into closer agreement, if the modified input or state is closer to the discharge in terms of the model structure. From this point of view, the modification of the UZ storage is the most effective procedure; however, note that this procedure acts much like replacing the simulated by the observed discharge and may not have a long lasting impact of the lead time performance of a forecast.

In a second step, we assess the sustainability of the different assimilation setups. It is obvious that the agreement of observed and simulated discharge is just one requirement for a suitable assimilation procedure. Another one is the sustainable impact of the assimilation in the streamflow forecast over the forecast horizon. Therefore, we implement a hindcasting experiment with alternating updating and forecast in daily intervals and a forecast horizon of 5 days over the validation period October 2009 – September 2012 (Table 11). In this step,

approximately same weights are provided to variables and discharges, moreover the increments of the bounds are restricted to the original values in Figure 5.

Table 11 Karasu: Model performance of simulation run without data assimilation in comparison to run with different data assimilation setups

Run	**Mean Flow**	**Lead Time Performance: RMSE [m³/s] (Oct 2009 – Sep 2012)**				**Lead Time Performance: R2 (Oct 2009 – Sep 2012)**			
	Q [m³/s]	1d	2d	3d	5d	1d	2d	3d	5d
without DA	81.84	34.07*	34.07*	34.07*	34.07*	0.746*	0.746*	0.746*	0.746*
DA (ΔP)	81.84	25.66	25.70	26.95	29.76	0.855	0.855	0.840	0.805
DA (ΔT)	81.84	46.66	46.71	47.41	48.69	0.740	0.745	0.736	0.713
DA (Δs_{SM})	81.84	20.61	21.81	23.53	26.84	0.930	0.922	0.906	0.871
DA (Δs_{UZ})	81.84	10.21	13.12	16.17	20.77	0.977	0.961	0.942	0.905
DA (Δs_{LZ})	81.84	25.25	24.94	26.46	29.03	0.859	0.862	0.843	0.811
DA (ALL)	81.84	9.63	12.77	16.03	21.30	0.979	0.964	0.944	0.901

* Since this value converges to the model performance, we set it equal to the value in Table 11.

The best performance for a modification of an individual term is obtained for the upper zone storage assimilation. The joint setup with a combination of all individual terms shows only a minor improvement compared to the single UZ setup.

3.4.2 Practical benefit of H-SAF products

The assessment of the practical benefit of the H-SAF data products is achieved by conducting hindcast experiment according to the setup in the previous section. Besides using only discharges as metrics for the agreement between the model and observations, we also include the H-SAF products H10 (snow covered area) and H13 (snow water extent) as additional metrics. The hindcast experiment is restricted to the years 2009-2012 for which the H-SAF snow products are available. Therefore, they are not directly comparable to the results of the previous section. Outcomes are summarized in Table 12.

Table 12 Model performance of simulation run without data assimilation in comparison to run with different data assimilation setups

Run	Mean Flow	Lead Time Performance: RMSE [m^3/s] (2009-2012)				Lead Time Performance: R2 (2009-2012)			
	Q [m^3/s]	1d	2d	3d	5d	1d	2d	3d	5d
H10-P/T/LZ	84.99	25.03	25.28	26.64	29.48	0.878	0.875	0.860	0.826
MODIS-P/T/LZ	84.99	25.67	25.98	27.83	30.94	0.873	0.869	0.846	0.804
H13-P/T/LZ	84.99	19.56	20.42	22.60	25.98	0.915	0.907	0.886	0.850
H10/13-P/T/LZ	84.99	26.50	26.78	28.23	30.70	0.855	0.853	0.836	0.804

H10 and Modis snow coverage products show a very similar performance in terms of model lead time performance. This is consistent with the close agreement of both products on a basin-averaged level (Figure 4). The DA with the H13 product shows better results than the ones with the snow covered area (H10/Modis). We believe that this results from the closer agreement between the H13 product and the HBV model states. In comparison, the snow covered area is a post-processed model output based on the simulated SWE of the lumped model (one basin, 10 elevation zones).

The use of both H10 and H13 in a DA run has approximately the performance of the run with H10 only and it is worse than the H13 run.

4 Conclusions and Recommendations

In this VSA, we implemented a test bed for assimilating several H-SAF products into the HBV hydrological model. It consists of the layers for i) data-model integration, ii) data assimilation, and iii) the hydrological model. All components are freely available or open source. The interface definition between the layers enables a replacement of one of the implemented components by a different one. In the specific implementation for the Karasu River basin, the MHE data assimilation and the HBV model relies on joint software, however, we also draft a generic setup for individual components.

The MHE setup for data assimilation in combination with the HBV model permits a joint assimilation of model forcing (precipitation, temperature) and model states (soil moisture, upper & lower zone storage) in combination with the comparison of observed and simulated quantities such as snow coverage, snow water equivalent, soil moisture and discharge. The overall test bed includes the MHE/HBV components in combination with processing features for the H-SAF products H10 and H13 as well as workflows and batch run definitions for conducting model calibration, data assimilation runs and hindcasting experiments.

The data assimilation setup turns out to be very flexible. It has many degrees of freedom. This is an attractive feature on the one hand, but it will probably require more detailed research on the parameterization of the approach for different basin types. The technical implementation of the framework led to many ad-hoc decisions on several issues which should be focus of further research. The most important ones include:

- The relation between snow water equivalents of the model, in this case a conceptual HBV model, and the fractional snow covered area.
- Criteria for the validation of the H-SAF data and the decision under which conditions, i.e. threshold for cloud coverage percentage in the basin, it should be considered in the assimilation.
- Metrics for defining the agreement between simulation and observation, so far only quadratic metrics have been used.

5 References

Andreadis, K.M. and Lettenmaier, D.P. (2006) Assimilating remotely sensed snow observations into a macroscale hydrology model, *Advances in Water Resources* 29(6), 872–886.

Andreadis, K. M., Clark, E. A., Lettenmaier, D. P., and Alsdorf, D. E. (2007) Prospects for river discharge and depth estimation through assimilation of swath-altimetry into a raster based hydrodynamics model, *Geophys. Res. Lett.*, 34, L10403, doi:10.1029/2007gl029721.

Aubert, D., Loumagne, C., and Oudin, L. (2003) Sequential assimilation of soil moisture and streamflow data in a conceptual rainfallrunoff model, *J. Hydrol.*, 280, 145–161, doi:10.1016/s0022-1694(03)00229-4.

Bales RC, Molotch NP, Painter TH, Dettinger MD, Rice R, Dozier J (2006) Mountain hydrology of the western United States. *Water Resour Res* 42. Doi: 10.1029/2005wr004387Brocca, L., Melone, F., Moramarco, T., Wagner, W., Naeimi, V.,

Bartalis, Z., and Hasenauer, S. (2010) Improving runoff prediction through the assimilation of the ASCAT soil moisture product, Hydrol. Earth Syst. Sci., 14, 1881–1893, doi:10.5194/hess-14-1881-2010.

Bergström S., The HBV model, In: Singh, V.P. (Ed.) Computer Models of Watershed Hydrology. Water Resources Publications, Highlands Ranch, CO., pp. 443-476, 1995

Boudhar, A., Hanich, L., Boulet, G., Duchemin, B., Berjamy, B., Chehbouni, A. (2009) Evaluation of the snowmelt runoff model in the Moroccan High Atlas Mountains using two snow-cover estimates. *Hydrological Science Journal*, 54(6), 1094-1113. doi:10.1623/hysj.54.6.1094

Butt, MJ and Bilal, M. (2011) Application of snowmelt runoff model for water resource management, *Hydrological Processes*, 25 (24) pg: 3735–3747,

Clark, M.P., Slater, A.G., Barrett, A.P., Hay, L.E., McCabe, G.J., Rajagopalan, B. and Leavesley, G.H. (2006) Assimilation of snow covered area information into hydrologic and land-surface models, *Advances in Water Resources* 29(8), 1209–1221.

Clark, M. P., Rupp, D. E., Woods, R. A., Zheng, X., Ibbitt, R. P., Slater, A. G., Schmidt, J., and Uddstrom, M. J.: Hydrological data assimilation with the ensemble Kalman filter: Use of streamflow observations to update states in a distributed hydrological model, *Adv. Water Resour.*, 31, 1309–1324, doi:10.1016/j.advwatres.2008.06.005, 2008.

De Lannoy, G. J. M., Reichle, R. H., Arsenault, K. R., Houser, P. R., Kumar, S., Verhoest, N. E. C., and Pauwels, V. R.N.: Multiscale assimilation of Advanced Microwave Scanning

Radiometer-EOS snow water equivalent and Moderate Resolution Imaging Spectroradiometer snow cover fraction observations in northern Colorado, *Water Resour. Res.*, 48, W01522, doi:10.1029/2011wr010588, 2012.

Derksen, C.P., Walker, A.E. and Goodison, B.E. (2003) A comparison of 18 winter seasons of in situ and passive microwave-derived snow water equivalent estimates in Western Canada, *Remote Sensing of Environment* 88(3), 271–282.

Dong, J., J. P. Walker, P. R. Houser, and C. Sun (2007) Scanning multichannel microwave radiometer snow water equivalent assimilation. *Journal of Geophysical Research*, 112 (D07108), D07 108.1–16, doi:10.1029/2006JD007209.

Dressler, K.A., Leavesley, G.H., Bales, R.C. and Fassnacht, S.R. (2006) Evaluation of gridded snow water equivalent and satellite snow cover products for mountain basins in a hydrologicmodel, *Hydrological Processes* 20(4), 673– 688.

Flores, A. N., Bras, R. L., and Entekhabi, D. (2012) Hydrologic data assimilation with a hillslope-scale-resolving model and L band radar observations: Synthetic experiments with the ensemble Kalman filter, *Water Resour. Res.*, 48, W08509, doi:10.1029/2011WR011500, 2012.

Gomez-Landesa, E. and A. Rango, (2002) Operational snowmelt runoff forecasting in the Spanish Pyrenees using the snowmelt runoff model. *Hydrological Processes*, 16, 1583-1591.

Griewank A., Walther A., Evaluating Derivatives, second edition. SIAM, 2008.

Hall, D.K. and Riggs, G.A. (2007) Accuracy assessment of the MODIS snow products, *Hydrological Processes* 21(12), 1534–1547.

Hall, D.K., Riggs, G.A., Foster, J.L. Kumar, S. (2010) Development and validation of a cloud-gap filled MODIS daily snow-cover product, *Remote Sensing of Environment*, 114:496-503, doi:10.1016/j.rse.2009.10.007

Immerzeel, W.W., Droogers, P., De Jong, S.M., Bierkens, M.F.P. (2009) Large- scale monitoring of snow cover and runoff simulation in Himalayan river basins using remote sensing, Remote Sensing of Environment, 113: 40- 49.

Jain SK, Goswami A, Saraf AK (2010) Snowmelt runoff modelling in a Himalayan basin with the aid of satellite data. *Int J Remote Sens* 31 (24): 6603-6618

Kolberg, S.A. and Gottschalk, L. (2006) Updating of snow depletion curve with remote sensing data, *Hydrological Processes* 20(11), 2363–2380.

Kolberg, S., Rue, H. and Gottschalk, L. (2006) A Bayesian spatial assimilation scheme for snow coverage observations in a gridded snow model, *Hydrology and Earth System Sciences* 10(3), 369–381.

Kumar, S.V., Peters-Lidard, C.D., Eastman, J.L., Kao, W.K. (2008) An integrated highresolution hydrometeorological modeling testbed using LIS and WRF. *Environmental Modelling & Software*, 23, 169–181.

Lee SW, Klein AG, Over TM (2005) A comparison of MODIS and NOHRSC snow-cover products for simulating streamflow using the Snowmelt Runoff Model. *Hydrol Process* 19 (15): 2951-2972. doi: 10.1002/Hyp.5810

Lee, H., Seo, D.J., Koren, V. (2011) Assimilation of streamflow and in situ soil moisture data into operational distributed hydrologic models: Effects of uncertainties in the data and initial model soil moisture states, *Adv. Water Resour.*, 34, 1597–1615, doi:10.1016/j.advwatres.2011.08.012.

Lindstrom G, Johannson B, Persson M, Gardelin M, Bergstrom S, Development and test of the distributed HBV-96 hydrological model, Journal of Hydrology 201, 272–288

Li, X. G., and Williams, M.W. (2008). Snowmelt runoff modeling in an arid mountain watershed, Tarim Basin, China. *Hydrological Processes*, 22(19), 3931-3940. doi:10.1002/hyp.7098

Liu, Y., Weerts, A.H., Clark, M., Hendricks Franssen, H.J., Kumar, S., Moradkhani, H., Seo, D.J., Schwanenberg, D., Smith, P., van Dijk, A.I J M., van Velzen, N., He, M., Lee, H., Noh, S.J., Rakovec, O., Restrepo, P. (2012) Advancing data assimilation in operational hydrologic forecasting: progresses, challenges, and emerging opportunities, *Hydrol. Earth Syst. Sci.*, 16, 3863–3887,doi:10.5194/hess-16-3863-2012.

Madsen, H., Butts, M.B., Khu, S.T., Liong, S.Y. (2000). Data assimilation in rainfall- runoff forecasting. *In: Proceedings of the Fourth International Conference on Hydroinformatics, Cedar Rapids*, Iowa, USA, 23–27 July.

Martinec J (1975) Snowmelt-runoff model for stream flow forecasts. *Nordic Hydrology* 6: 145-154.

Martinec J, Rango A, Major E. (1983) The Snowmelt-Runoff Model (SRM) User's Manual. *NASA Reference Publication No. 1100*. NASA:Washington, DC.

Martinec, J., Rango, A., Roberts, R.T. (2008) *Snowmelt Runoff Model (SRM) User's Manual*, 19-39. New Mexico: New Mexico State University Press.

McGuire M, Wood AW, Hamlet AF, Lettenmaier DP (2006) Use of satellite data for streamflow and reservoir storage forecasts in the snake river basin. *J Water Res Pl*-Asce 132 (2): 97-110. doi: 10.1061/(Asce)0733-9496

McMillan H.K.. Hreinsson, E.O., Clark, M.P., Singh, S.K., Zammit, C., Uddstrom, M. J. (2013) Operational hydrological data assimilation with the recursive ensemble Kalman filter *Hydrol. Earth Syst. Sci.*, 17, 21–38 doi:10.5194/hess-17-21-2013

McLaughlin, D. (1995) Recent advances in hydrologic data assimilation, US Natl Rep Int Union Geod Geophys 1991–1994. *Rev Geophys*; 33:977–84.

Mitchell, K. M. and D. R. DeWalle (1998) Application of the snowmelt runoff model using multiple-parameter landscape zones on the Towanda Creek Basin, Pennsylvania. *JAWRA*, 34, 335-346.

Neal, J., Schumann, G., Bates, P., Buytaert, W., Matgen, P., Pappenberger, F. (2009) A data assimilation approach to discharge estimation from space, *Hydrol. Process.*, 23, 3641–3649, doi:10.1002/hyp.7518.

Nagler, T., Quegan, S. Rott, H. (2008) Assimilation of meteorological and remote sensing data for snowmelt runoff forecasting. *Remote Sensing of Environment*, 112, 1408-1420.

Parajka, J., Naeimi, V., Blöschl, G., Wagner, W., Merz, R., Scipal, K. (2006) Assimilating scatterometer soil moisture data into conceptual hydrologic models at the regional scale, *Hydrology and Earth System Science*, 10, 353-368

Parajka, J. and Blöschl, G. (2008) The value of MODIS snow cover data in validating and calibrating conceptual hydrologic models, *Journal of Hydrology*, 358, 240-258.

Pulliainen, J. (2006) Mapping of snow water equivalent and snow depth in boreal and sub-arctic zones by assimilating space-borne microwave radiometer data and ground-based observations, *Remote Sensing of Environment* 101(2), 257–269.

Rango A, Martinec J. (1995) Revisiting the degree-day method for snowmelt computations. *Water Resources Bulletin* 31(4): 657–669.

Rango, A. and Katwijk, V.V. (1990) Development and Testing of a Snowmelt-Runoff Forecasting Technique. *Water Resources Bulletin*, 26, 135-144.

Reichle, R.H. (2008) Data assimilation methods in the Earth sciences, *Adv. Water Res.*, 31, 1411–1418, doi:10.1016/j.advwatres.2008.01.001.

Richard, C. and Gratton, D.J. (2001) The Importance of the air temperature variable for the snowmelt runoff modeling using the SRM. *Hydrological Processes*, 15, 3357–3370.

Rodell, M., and Houser P.R. (2004) Updating a land surface model with MODIS- derived snow cover, J. Hydrometeorol., 5, 1064–1075.

Schwanenberg, D.: HBV Replacement Project, University of Duisburg-Essen, November 2012 (unpublished)

Schwanenberg D, Sheret I, Rauschenbach T, Galelli S, Vieira JM, Pinho JL: Adjoint Modelling Framework, 10th Conf. Hydroinformatics HIC2012, 14-18 July 2012, Hamburg, Germany

Schwanenberg D., Becker B., RTC-Tools Reference Manual, Deltares, 2014

Schmugge, T.J., Kustas, W.P., Ritchie, J.C., Jackson, T.J. and Rango, A. (2002) Remote sensing in hydrology. *Advances in Water Resources* 25:1367-1385.

Seo, D., Koren, V., Cajina, N. (2003) Real-time variational assimilation of hydrologic and hydrometeorological data into operational hydrologic forecasting. *J. Hydromet*. **4**, 627–641.

Slater, A.G. and Clark, M.P. (2006) Snow data assimilation via an ensemble Kalman filter, *J. Hydrometeorol.*, 7, 478–493, doi:10.1175/jhm505.1.

Su, H., Yang, Z.L., Niu, G.Y., Dickinson, R.E. (2008) Enhancing the estimation of continentalscale snow water equivalent by assimilating MODIS snow cover with the ensemble Kalman filter, *J. Geophys. Res.*, 113, doi:10.1029/2007JD009232, 2008. 1331, 1333, 1338.

Şensoy A., Uysal G. (2012) The Value of Snow Depletion Forecasting Methods Towards Operational Snowmelt Runoff Estimation Using MODIS and Numerical Weather Prediction Data, *Water Resources Management*, 26, pp.3415-3440, DOI 10.1007/s11269-012-0079-0

Şensoy A., Şorman A.Ü., Şorman A.A. (2012) Comment on "Catchment flow estimation using Artifical Neural Networks in the mountainous Euphrates basin" by A.G. Yilmaz, M.A. Imteaz, G. Jenkins (J. Hydrol. 410 (2011) 134–140) *Journal of Hydrology*, Vol. 454–455, pp.208-210, DOI 10.1016/j.jhydrol.2012.05.067

Şensoy A, Şorman AA, Tekeli AE, Şorman AÜ, Garen DC (2006) Point-scale energy and mass balance snowpack simulations in the upper Karasu basin, Turkey. *Hydrol Process* 20 (4): 899-922. doi: 10.1002/Hyp.6120

Şorman AA, Şensoy A, Tekeli AE, Şorman AÜ, Akyürek Z (2009) Modelling and forecasting snowmelt runoff process using the HBV model in the eastern part of Turkey. *Hydrol Process* 23 (7): 1031-1040. doi: 10.1002/Hyp.7204

Şorman A.Ü., Beser Ö. (2012) Determination of snow water equivalent over the eastern part of Turkey using passive microwave data *Hydrol Process*. doi: 10.1002/hyp.9267

Şorman A.Ü., Akyürek Z., Şensoy A., Şorman A.A., Tekeli A.E. (2007) Commentary on comparison of MODIS snow cover and albedo products with ground observations over the mountainous terrain of Turkey *Hydrological Earth System Science*, 11, pp.1353-1360, DOI 10.5194/hess-11-1353-2007

Tahir, A.A., Chevallier, P., Arnaud, Y., Neppel, L., Ahmad, B. (2011). Modeling snowmelt-runoff under climate scenarios in the Hunza River basin, Karakoram Range, Northern Pakistan. Journal of Hydrology, In Press, Accepted Manuscript. doi: 10.1016/j.jhydrol.2011.08.035.

Tekeli, A.E., Akyürek, Z., ¸Sorman, A.A., Sensoy, A., Sorman, A.Ü. (2005) Using MODIS snow cover maps in modeling snowmelt runoff process in the eastern part of Turkey, *Remote Sensing of Environment* 97(2), 216–230.

Udnaes, H.C., Alfnes, E., Andreassen, L.M. (2007) Improving runoff modelling using satellite-derived snow covered area, *Nordic Hydrology* 38(1), 21–32.

Wächter A. and Biegler L.T., On the Implementation of a Primal-Dual Interior Point Filter Line Search Algorithm for Large-Scale Nonlinear Programming, Mathematical Programming 106(1), pp. 25-57, 2006

Weerts A, El Serafy GY, Hummel S, Dhondia J, Gerritsen H, Application of generic data assimilation tools (DATools) for flood forecasting purposes, Computers & Geosciences 36(2010) 453–463

WMO (1986) Intercomparison of Models of Snowmelt Runoff, Geneva, Switzerland.

WMO (1992) Simulated Real-time Intercomparison of Hydrological Models, Geneva, Switzerland.

Xingong, L. and Williams, M. W. (2008) Snowmelt runoff modelling in an arid mountain watershed,Tarim Basin, China. *Hydrol. Processes* **22**, 3931–3940.

Yang, D., Robinson, D., Zhao, Y., Estilow, T. and Ye, B. (2003) Streamflow response to seasonal snow cover extent changes in large Siberian watersheds, *Journal of Geophysical Research D: Atmospheres* 108(D18), 4578 ACL–7 1–14.

Werner, M.G.F., van Dijk, M., Schellekens, J. (2004) DELFT-FEWS: an open-shell flood forecasting system. In: Liong, S.Y., Phoon, K., Babovic, V. (Eds.), *Proceedings of the Sixth International Conference on Hydroinformatics*, World Scientific Publishing Company, pp. 1205–1212, ISBN 981-238-787-0.

Werner, M.G.F., Heynert, K. (2006) Open model integration – a review of practical examples in operational flood forecasting. In: Gourbesvile, P., Cunge, J., Guinot, V., Liong, S.Y. (Eds.), *Proceedings of the Seventh International Conference on Hydroinformatics*, vol. I, Research Publishing, pp. 155–162, ISBN 819-031-702-4.

Werner, M., Schellekens, J., Gijsbers, P., van Dijk, M., and van den Akker, O., Heynert, K (2013) The Delft-FEWS flow forecasting system, *Environ. Model. Softw.*, 40, 65-77.

Zaitchik, B.F. and Rodell, M. (2009) Forward- looking assimilation of MODIS- derived snow covered area into a land surface model, J. Hydrometeorol., 10(1), 130–148, doi:10.1175/2008JHM1042.1.

Zhou, H.Y., Gomez-Hernandez, J.J., Franssen, H.J.H., Li, L.P. (2011) An approach to handling non-Gaussianity of parameters and state variables in ensemble Kalman filtering, *Adv. Water Resour.*, 34, 844–864, doi:10.1016/j.advwatres.2011.04.014.

Appendix A – Procedure for Running the Experiments

Model Calibration and validation:

1) Delete the local data store (close the application and delete the folder "…\regionHome\localDataStore\").
2) Copy the Karasu data ("PTEQ_Karasu2000-12.csv") from the "…\regionHome\ImportBackup\ExcelCSV_Daily\" to the "…\regionHome\Import\ExcelCSV_Daily\" folder.
3) Run the "HBV_Karasu_UpdateD.xml" batch script from the Manual Forecast Display

Step 1A:

1) Delete the local data store (close the application and delete the folder "…\regionHome\localDataStore\").
2) Copy the Karasu data ("PTEQ_Karasu2000-12.csv") from the "…\regionHome\ImportBackup\ExcelCSV_Daily\" to the "…\regionHome\Import\ExcelCSV_Daily\" folder.
3) Select one of the modifiers from the Modifier Display. Therefore, Click the "HBV_Karasu_UpdateD_DA" entry in the Interactive Forecasting Display and select "Create mod", then choose one of the available "Step 1 …" modifiers and apply it. Make sure that only one modifier is active at the same time.
4) Run the "HBV_Karasu_UpdateD_DA.xml" batch script from the Manual Forecast Display

Step 1B:

1) Repeat steps 1)-3) of the Step 1A procedure above.
2) Run the "HBV_Karasu_Hindcast_DA.xml" batch script from the Manual Forecast Display